ESTIMATING VERTICAL LEAF AREA DENSITY PROFILES OF TREE CANOPIES USING THREE-DIMENSIONAL PORTABLE LIDAR IMAGING

F. Hosoi, K.Omasa

Graduate School of Agricultural and Life Sciences, The University of Tokyo, Yayoi 1-1-1, Bunkyo-ku, Tokyo 113-8657, Japan- aomasa@mail.ecc.u-tokyo.ac.jp

KEY WORDS: Broad leaf, Canopy**,** Leaf area density, Lidar, Point cloud, 3D, Voxel

ABSTRACT:

In this paper, a new method for estimation of vertical leaf area density (LAD) profile of tree canopy using portable scanning lidar is proposed. In this method, which we refer to as the voxel-based canopy profiling (VCP) method, several measurement points surrounding the canopy and optimally inclined laser beams are adopted to facilitate full laser beam illumination of whole canopy up to the internal. After the scanning, each data obtained from each measurement point are co-registered and the 3-D information is reproduced as the voxel attributes in the 3-D voxel array. Based on the voxel attributes, contact frequency of laser beams on leaves is computed and LAD in each horizontal layer is obtained. In addition, influence of non-photosynthetic tissues and leaf inclination angle on the LAD estimation are corrected. Using the method, good agreement between estimated and actual LAD was obtained in an individual tree of *Camellia sasanqua*. Next, the method was applied to broad leaved woody canopy of Japanese zelkova (*Zelkova serrata* (Thunb.) Makino). In the experiment, LAD profiles had different accuracy depending on each quadrat established on the measurement plot and on the laser incident angles. From the results, it was shown that the number of laser beam incidences *N* and $G(\theta_c)$ (the mean projection of a unit leaf area on a plane perpendicular to the direction of the laser beam) are the factors to influence the accuracy of LAD estimation.

1. INTRODUCTION

The plant canopy plays important functional roles in cycling of materials and energy through photosynthesis and transpiration, maintaining plant microclimates, and providing habitats for various species. Determining the vertical structure of the canopy is thus very important because the three-dimensional (3D) composition of the canopy helps to sustain those functional roles. Researchers often represent the vertical foliage structure using the leaf area density (LAD) in each horizontal layer, where LAD is defined as the total one-sided leaf area per unit of layer volume. The leaf area index (LAI), which is defined as the leaf area per unit of ground area covered by the projected area of the crown, is then calculated by vertically integrating the LAD profile data.

Although there are several ways to measure LAD and LAI, these measurements remain difficult. Stratified clipping of biomass samples is one direct measurement method. However, its application in the field is limited because of its destructive and laborious nature. Indirect methods have thus become a popular alternative. The first indirect method that was developed is the point-quadrat method (Warren-Wilson, 1960), in which a probe with a sharp point is inserted into the canopy at a known inclination and azimuth angle, and the number of times the point contacts leaves or stems is counted. LAD and LAI can then be estimated by calculating the contact frequency. However, this method is also very laborious (Norman and Campbell, 1989). Another indirect method, the gap-fraction method, is widely applied in field surveys and uses commercially available tools such as cameras with a fish-eye lens and optical sensors (e.g., the LI-COR LAI-2000 Plant Canopy Analyzer; Norman and Campbell, 1989). This method allows automatic estimation of LAI or LAD without destruction of the plants and is less laborious. However, it depends on the assumption that the foliage distribution is random, which leads to the errors when the foliage distribution is nonrandom.

Recently, lidar (light detection and ranging) has been applied to canopy measurements (Omasa et al., 2000, 2003, 2007; Hyyppä et al, 2001; Lefsky et al., 2002; Popescu et al., 2003; Næsset et al., 2004; Hosoi and Omasa, 2006, 2007, 2009). Portable ground-based scanning lidar has been utilized to obtain plant structural properties such as canopy height, above ground biomass (Radtke and Bolstad, 2001; Omasa *et al.,* 2007). Portable scanning lidar has several beneficial features for LAD and LAI measurements. For instance, it is nondestructive and, because it is an active sensor, measurements are not affected by the light conditions in the field. The high ranging accuracy and fine resolution allow to capturing detailed structural information of a canopy. In addition, it can record many 3-D data for a canopy quickly and automatically as 3-D point-cloud data. Thus, this technology promises to overcome the shortcomings of the conventional means of measuring LAD profile of the canopy.

Based on the features, we developed a practical method for accurate LAD estimation of a canopy using portable scanning lidars, which we refer to as the voxel-based canopy profiling (VCP) method. In this paper, the methodology and the applications to an individual tree and broad-leaved canopy are presented.

2. METHODS

2.1 3-D data acquisition and registration

In the VCP-method, several measurement points surrounding the canopy and optimally inclined laser beams are adopted. This setting facilitates full laser beam illumination of whole canopy up to the internal (Fig.1(a)). The measurements offer accurate

and precise 3-D point cloud images of whole canopy. The complete data set is composed of several point cloud data, one obtained from each of the several measurement positions. These data with their individual coordinate systems are registered into a single-point cloud data set with a common coordinate system by using the iterative closest point algorithm (Besl and McKay, 1992).

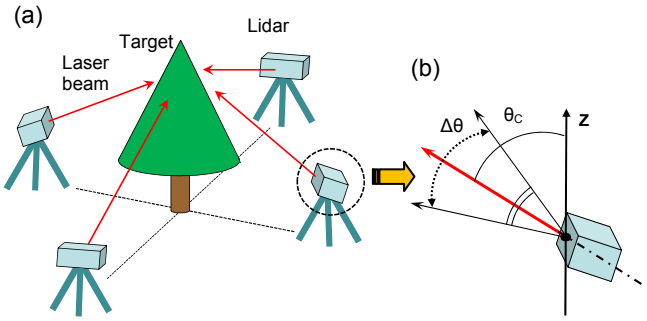

Figure 1: Schematic illustrations of lidar measurements (the case in an individual tree).(a): Typical lidar positions around a target tree. (b): Laser beam inclination represented by the central zenith angle of laser beam (θ_c) and the zenith scan angle ($\Delta\theta$).

2.2 Removal of non-photosynthetic tissues

In addition to the leaved canopy measurement, the leafless canopy is also measured and the data are co-registered by the similar ways as above described. Non-photosynthetic tissues such as trunks and branches are excluded by subtracting the leafless image from the leaved one.

2.3 Voxelization

A voxel is defined as a volume element in a 3D array. All points within the registered data are converted into voxel coordinates by the following equations.

$$i = Int\left(\frac{X - X_{\min}}{\Delta i}\right)+1, \quad j = Int\left(\frac{Y - Y_{\min}}{\Delta j}\right)+1, \quad k = Int\left(\frac{Z - Z_{\min}}{\Delta k}\right)+1 \qquad (1)$$

where (i, j, k) represents the voxel's coordinates within the voxel array, *Int* is a function that rounds off the result of the calculation to the nearest integer, (X, Y, Z) represents the point coordinates of the registered lidar data, ($X_{\min}$, $Y_{\min}$, $Z_{\min}$) represent the minimum values of (X, Y, Z) and (Δi, Δj, Δk) represent the voxel element size. The voxel element size is determined, dependeding on the range and scan resolution of the lidar (e.g., ΔI = Δj = Δk =1mm, in the case of high-resolution lidar with the resolution of about 1mm). Voxels corresponding to coordinates converted from points within the registered data are assigned 1 as the attribute value. A voxel with the attribute value of 1 represents a voxel in which at least one laser beam is intercepted by leaves. All laser beams emitted from the lidar positions are then traced within the voxel array in accordance with the actual laser beam angles (see Fig.2). If voxels that do not have an attribute value of 1 are intersected by at least one laser beam trace, the voxel was assigned 2 as the attribute value. A voxel with an attribute value of 2 therefore represents a voxel through which one or more laser beams passed without touching a leaf. Other voxels that are assigned neither attribute value are omitted from the following LAD computation.

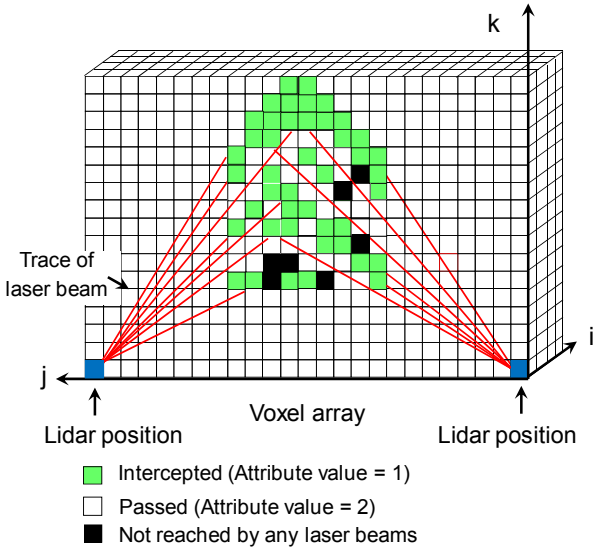

Figure 2: Schematic illustration of assignment of voxel attributes (Lidar positions were placed in the corners for better visualization of laser beam traces).

2.4 LAD computation

Based on the attribute values, LAD is computed in each horizontal layer of the canopy using the following equation:

$$\mathrm{LAD}(h,\Delta H) = \frac{\cos\theta}{G(\theta)} \cdot \frac{1}{\Delta H} \sum_{k=m_h}^{m_{h+\Delta H}} \frac{n_1(k)}{n_1(k)+n_P(k)} \qquad (2)$$

where θ is the zenith angle of a laser beam, ΔH is the horizontal layer thickness, and m_h and $m_{h+\Delta H}$ are the voxel coordinates on the vertical axis equivalent to height h and $h+\Delta H$ in orthogonal coordinates ($h = \Delta k \times m_h$). $n_I(k)$ and $n_P(k)$ are the numbers of voxels with the attribute values of 1 and 2 in the kth horizontal layer of the voxel array, respectively. Thus, $n_I(k) + n_P(k)$ represent the total number of incident laser beams that reach the kth layer and $n_I(k)/(n_I(k) + n_P(k))$ represents contact frequency of laser beams on the canopy. $G(\theta)$ is the mean projection of a unit leaf area on a plane perpendicular to the direction of the laser beam at θ (Norman and Campbell, 1989). The term $\cos(\theta)[G(\theta)]^{-1}$ is a correction factor for the influence of leaf inclination angle and laser beam direction. Eq.(2) is analogous to the equation of radiation transfer through canopy in the case of neglecting the scattering term (Ross, 1981). $n_I(k) + n_P(k)$ and $n_I(k)$ in Eq.(2) correspond to the radiation intensity and the attenuation of the radiation intensity in the radiation transfer equation. $\cos(\theta)[G(\theta)]^{-1}$ is determined using the distribution of leaf inclination angles. Also, constant value of 1.1 can be chosen for $\cos(\theta)[G(\theta)]^{-1}$ in the case of the laser beam angle of 57.5°, at which the value can be considered nearly independent of leaf inclination (Warren-Wilson, 1960).

3. EXPERIMENTS

3.1 LAD estimation for an individual tree

At the first step, we tested our VCP-method on an individual tree of *Camellia sasanqua* with the height of 1.60m (Hosoi and Omasa, 2006). A fine-resolution portable scanning lidar (TDS-130L 3D laser scanner, Pulstec Industrial Co., Ltd), that

calculates distances based on trigonometry, was used for the measurement. The range accuracy was about 2 mm, and the scan resolution was about 1 mm. A rotating mount run by a built-in stepping motor and a galvano-mirror within the lidar head facilitated horizontal and vertical scanning by the instrument. Four azimuth symmetrical lidar positions were set around the specimen (see Fig.1(a)) and 3-D point cloud data in each position were recorded. Several central zenith angles of laser beams (the definition is in Fig.1(b)) from 37.5 to 180 ° were tried to know the optimum angle. After the lidar measurements, voxelization was conducted with the voxel size of 1 mm × 1 mm × 1 mm and LAD was computed. For obtaining validation data, actual LAD and LAI values in each horizontal layer of the specimen were measured by stratified clipping after the lidar measurements.

Figure 3 shows the co-registered 3-D point cloud lidar image. As shown in the image, the whole canopy was reproduced precisely at the individual leaf scale. The best result of LAD estimation was obtained at the central zenith angle of laser beam of 57.8 ° as shown in Fig.4. Good agreement between the estimate and the actual was observed in the result with the mean absolute percent error (MAPE) of 17.4%.

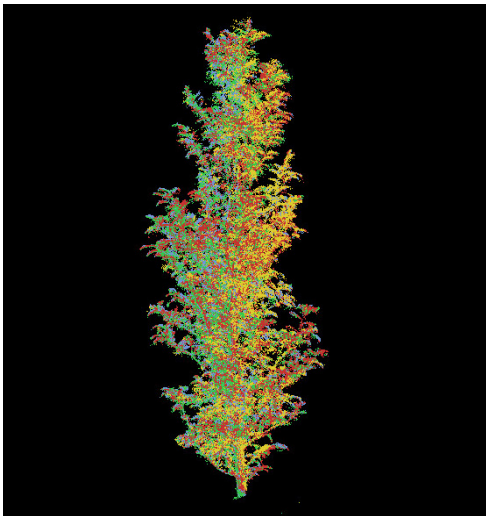

Figure 3: Co-registered 3-D point cloud lidar image of *Camellia sasanqua*. Each color (R,G,B,Y) represents data obtained from each measurement positions.

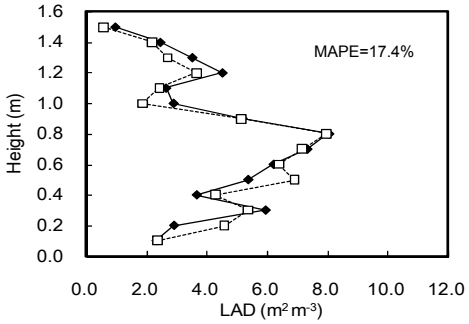

Figure 4: Comparison of LAD profiles for *C. sasanqua* between the lidar-derived estimates (white square) and actual values (black square). MAPE=mean absolute percent error (Hosoi and Omasa, 2006).

The corresponding LAI absolute error was 0.7 %. In addition, the optimum angle of 57.8 ° was beneficial because the value was near to the particular angle of 57.5 ° above described , and thus the constant value of 1.1 could be given for the correction factor of $\cos(\theta)[G(\theta)]^{-1}$ without using leaf inclination angle data. The optimum angle could have a different value depending on canopy structure. In the case of the optimum angle different from the particular angle of 57.5 °, leaf inclination angle data is required for the LAD computation.

3.2 LAD estimation for broad-leaved woody canopy

At the next step, the VCP-method was applied to broad-leaved woody canopy. In the experiment, the LAD estimates were first compared with actual values to validate the approach. The factors that contributed to the accuracy of the estimates were then investigated (Hosoi and Omasa, 2007).

The experiment was conducted in a mixed plantation in Ibaraki Prefecture, 40 km northeast of central Metropolitan Tokyo, Japan. The topography was nearly flat. A 4 × 8-m measurement plot was established at the site (Fig. 5 (a)), and the Japanese zelkova canopy within the plot was used for the experiment. The plot was divided into eight 2 × 2-m quadrats (Fig. 5 (b)) and each vertical region within each of the quadrats was divided into 16 cells (each 2 × 2 × 0.5 m) between heights of 5 to 13 m above the ground, as shown in Fig. 6. The entire canopy within the measurement plot was thus divided into 128 cells.

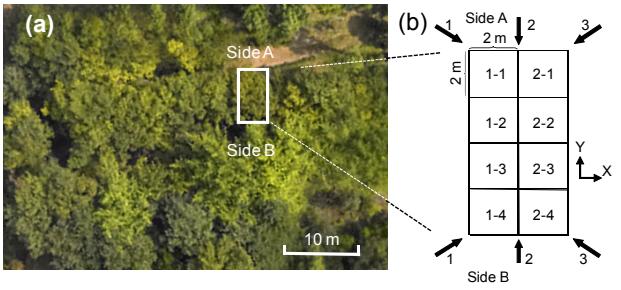

Figure 5: Study area. (a):Aerial photograph (b): A measurement plot established beneath the zelkova canopy. Arrows in (b) show the directions in which lidar scanning was performed (modified from Hosoi and Omasa, 2007).

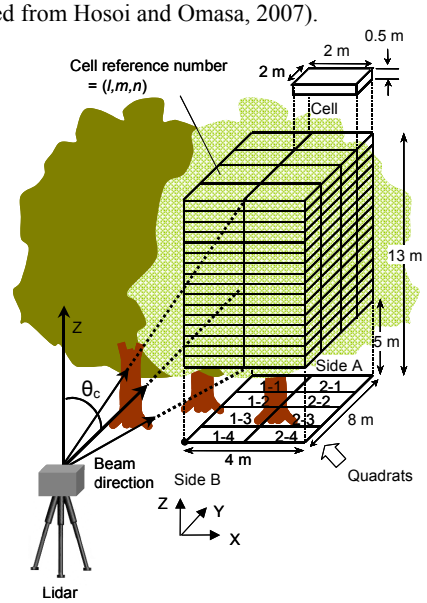

Figure 6: Illustration of the cells established within the measurement plot. θ_c: the central zenith angle of laser beam (modified from Hosoi and Omasa, 2007).

To measure the leaf inclination angle, the canopy within the measurement plot was scanned by the same portable high resolution scanning lidar as used in section 3.1. Each leaf was distinguishable from the acquired 3D point cloud image because of the fine resolution (see Fig.7). After randomly selecting 200 leaves in the image, each leaf was manually extracted and approximated as a plane and normals to the planes were estimated. The distribution of leaf inclination angles was derived from the angles of these normals with respect to the zenith (see Fig.8).

Figure 7: Close-up view of the 3-D point cloud image of Japanese zelkova canopy taken by high-resolution portable scanning lidar.

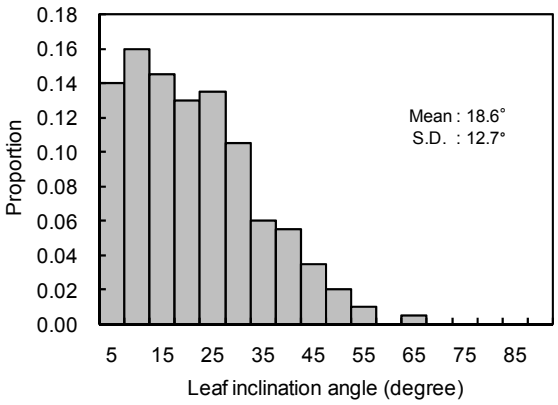

Figure 8: Distribution of leaf inclination angles in Japanese zelkova canopy derived from a high-resolution portable scanning lidar image (Fig.7) (Hosoi and Omasa, 2007).

Another type of portable scanning lidar (LPM-25HA, RIEGL, Austria) was used for the application of the VCP method. The portable lidar was able to obtain the distance to the surface of an object between 2 and 60 m from the sensor by measuring the elapsed time between the emitted and returned laser pulses (the "time of flight" method). The lidar had an accuracy of ± 8 mm when computing the range of each sample point. The Japanese zelkova canopy within the measurement plot was scanned by the lidar from several ground positions (see Fig. 5 (b)) in August 2005. The central zenith angles of the laser beams θ_c (Fig. 6) was 47.2º, 57.8º, and 71.3º at each measurement position. The canopy was also measured from positions 10 m above the ground using a cherry picker. The central zenith angle of the laser beams was 90.0º (i.e., horizontal direction). After the measurements during the leafy condition in August 2005, the same canopy was measured from the ground in February 2006, during the leafless condition. After the registration in each of the lidar-data sets, non-photosynthetic tissues and understory were excluded by extracting corresponding points between the 3D lidar data in the leafless condition and the one in the leafy condition. Then, voxelization process was applied in each angle data and LAD in each cell within the measurement plot was computed using following equation.

$$\mathrm{LAD}_{lmn} = \frac{\cos\theta_{lmn}}{G(\theta_{lmn})} \cdot \frac{1}{\Delta H} \sum_{k=m_h}^{m_{h+\Delta H}} \frac{n_1(k)}{n_1(k)+n_P(k)}. \quad (3)$$

where (l, m, n) represents the cell reference number, θ_{lmn} is the mean zenith angle for all laser beam incidences within a cell, ΔH is the vertical thickness of a cell (= 0.5 m). Other parameters are same in Eq.(2). This equation is modification of Eq.(2) for LAD computation of each cell. The correction factor $\cos(\theta_{lmn})[G(\theta_{lmn})]^{-1}$ was calculated from the leaf inclination angle distribution obtained by high-resolution lidar described above (Fig. 8).

Figure 9 shows 3D lidar images of the zelkova canopy after registration of the images. Trees in the measurement plot were extracted as shown in Figure 9(b-1) from the overall image shown in Figure 9 (a), and then the non photosynthetic tissues, including undergrowth (Fig. 9 (b-2)) and the leaves (Fig.9(b-3)) were separated. Each tissue was clearly distinguishable because of the fine resolution of the images.

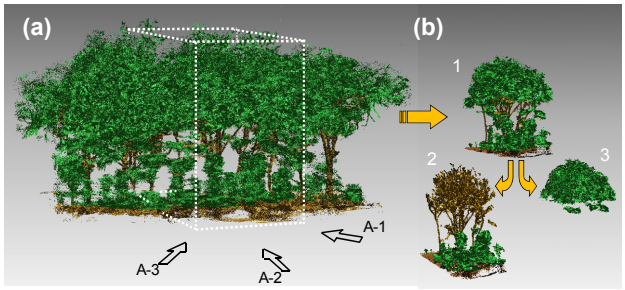

Figure 9: Co-registered 3-D point cloud lidar images of the Japanese zelkova canopy at this site. (a): A section of the canopy. The area enclosed by the white broken line corresponds to the measurement plot. (b) : Separation of the image into its components. (1): Trees in the measurement plot. (2):Separation of non-photosynthetic tissues including undergrowth. (3) Separation of leaves (Hosoi and Omasa, 2007).

The lidar-derived LAD profiles were compared with the actual stratified clipping values. Figure 10 shows the examples of the LAD profiles. The estimates for quadrat 1-1 (Fig. 10(a)), which was close to the lidar position on side A (see Fig.5(b)), showed good agreement with the actual values at all central zenith angles, while the LAD estimates at quadrat 2-3 underestimated the actual values at greater heights, except at a central angle of 90.0º (Fig. 10 (b)); this quadrat was in the middle of the measurement plot. The same tendency was observed in the other quadrats; that is, the closer the quadrats were to the lidar positions, the smaller the underestimation of the actual LAD value, except at the 90.0º central angle. The mean root mean square errors (RMSEs) of the LAD estimates for each quadrat were 0.50, 0.64, 0.78, and 0.44 m^2 m^{-3} at central zenith angles of 47.2, 57.8, 71.3, and 90.0º, respectively. The mean absolute errors of LAI for each quadrat were 21, 37, 57, and 12.7% at angles of 47.2, 57.8, 71.3, and 90.0°, respectively. More laser beams could reach the quadrats close to the lidar positions, compared with the ones in the middle of the measurement plot

because path length of the laser beam was shorter at the former quadrats than the latter ones

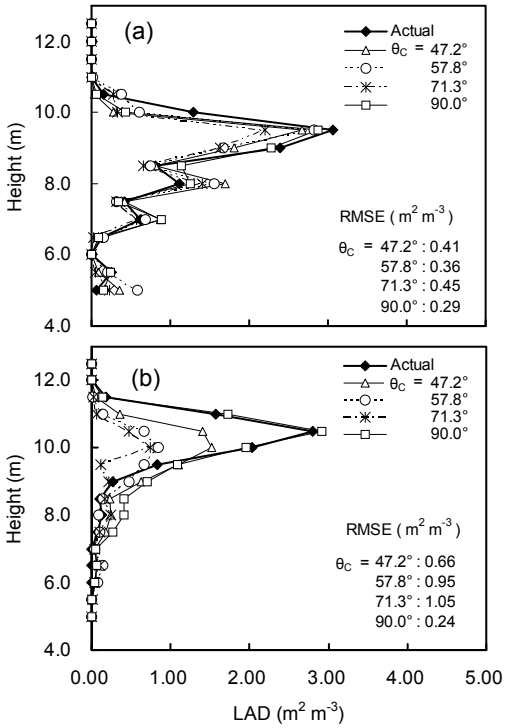

Figure 10: Comparison of LAD profiles in two quadrats between the lidar-derived estimates with different central zenith angles (θ_c) and the actual value. (a) Quadrat 1-1 and (b) quadrat 2-3 (Hosoi and Omasa, 2007).

This would have caused the difference in LAD estimation accuracy among quadrats. The relationship between the LAD estimation accuracy and the number of incident laser beams (N) is shown in Fig. 11, in which larger N offers less RMSE of LAD for all zenith angles. In addition, it was observed that the slope of the regression lines in Fig.11 increases as the central zenith angle increases. In particular, the rate of decrease of RMSE with increasing N is higher at the 90.0° angle than at the other angles. This means that the 90.0° angle offers more accurate estimates than the other angles when the value of N exceeds a certain value, i.e., $N > 0.3 \times 10^4$ incidences m^{-3}, estimated from the intersection points of the regression lines in Fig. 11(a) to (d). This explains the better LAD estimates at the 90.0° angle then the other angles because N exceeded 0.3×10^4 incidences m^{-3} at most of the cells.

The relationships in Figure 11 were fitted well using a power function:

$$\mathrm{RMSE} = aN^b \tag{4}$$

This function is characterized by the coefficient a and the scaling exponent b. Figure 11 indicates that a increased and b decreased as the central zenith angle increased. We hypothesized that the change in a and b for each central zenith angle relates to the change in $G(\theta_c)$ that accompanies the increase in the central zenith angle. Then, we calculated $G(\theta_c)$ in each central zenith angle by using leaf inclination angle distribution data and related the result to the corresponding values of a and b. As shown in Figure 12(a) for coefficient a and Figure 12(b) for the scaling exponent b, the resulting relationships could be expressed as functions of $G(\theta_c)$ as follows:

$$a = -22.484\ln[G(\theta_c)] - 5.808, \quad b = 0.183\ln[G(\theta_c)] - 0.171 \tag{5}$$

From Eqs. (4) and (5), the RMSE at each central zenith angle was expressed as a common function of N and $G(\theta_c)$. Here, a possible reason why $G(\theta_c)$ is one of factors to affect LAD estimation accuracy is the presence of obstructed leaves. In this context, "obstructed" refers to leaves that the laser beams cannot reach as a result of obstruction by other leaves. The presence of these leaves causes an error in LAD estimation, and the degree of obstruction would differ among the central zenith angles. The degree of the obstruction might be assessed by projection of leaf area on a plane perpendicular to the direction of the laser beam. The mean is $G(\theta_c)$, and thus $G(\theta_c)$ would affect the estimation accuracy.

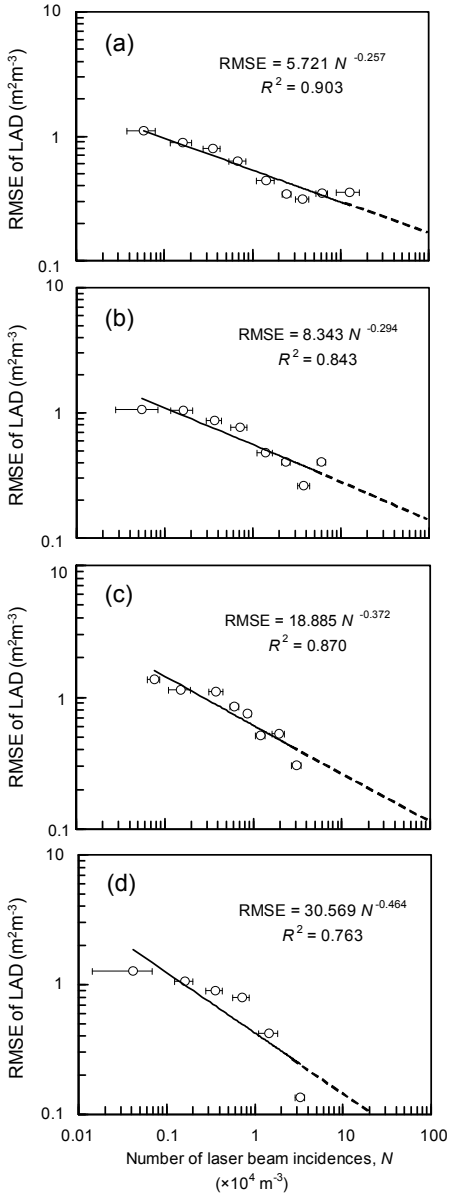

Figure 11: Relationships between the root-mean-square error (RMSE) of the LAD estimates and the number of laser beam incidences in each cell (N). The central zenith angles are (a) 47.2º, (b) 57.8, (c) 71.3º, and (d) 90.0º. Error bars are standard deviations (Hosoi and Omasa, 2007).

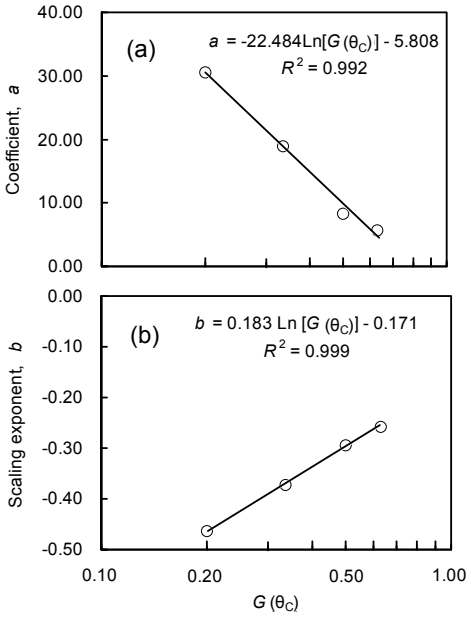

Figure 12: Relationship between the mean projection of a unit leaf area on a plane perpendicular to the direction of the laser beam at θ_c ($G[\theta_c]$) and the parameters *a* and *b* in Eq. (5). (a) $G(\theta_c)$ vs. coefficient *a*. (b) $G(\theta_c)$ vs. scaling exponent *b*. θ_c represents the central zenith angle (Hosoi and Omasa, 2007).

4. CONCLUSIONS

The VCP method for accurate estimation of LAD was demonstrated using portable scanning lidars. The essential points of the method are: (1) determining measurement positions that surround a target tree (2) Optimizing laser beam incident angle (3) Voxelization of obtained lidar data and computation contact frequency of laser beams on leaves based on the attributes of voxels (4) Correction of non-photosynthetic tissues and leaf inclination angle. Based on the method, good agreement between estimated and actual LAD was obtained in the individual tree. The method was also applied to the canopy of broad leaved trees. In the experiment, estimated LAD profiles had different accuracy depending on each quadrat established on the measurement plot and on the laser incident angles. From the results, it was shown that the number of laser beam incidences *N* and G(θc) (the mean projection of a unit leaf area on a plane perpendicular to the direction of the laser beam) are the factors to influence the accuracy of LAD estimation. By considering these factors in the lidar measurements, more accurate LAD estimates can be obtained. In the future, more works should be conducted for more species, in particular coniferous species or crops, to well take advantage of the present method.

5. REFERENCES

Besl, P.J., McKay, N.D., 1992. A method for registration of 3-D shapes. IEEE Transactions on Pattern Analysis and Machine Intelligence 14 (2), 239-256.

Hosoi, F., Omasa, K., 2006. Voxel-based 3-D modeling of individual trees for estimating leaf area density using high-resolution portable scanning lidar. *IEEE Transactions on Geoscience and Remote Sensing,* 44 (12), pp.3610-3618.

Hosoi, F., Omasa, K., 2007. Factors contributing to accuracy in the estimation of the woody canopy leaf-area-density profile using 3D portable lidar imaging. *Journal of Experimental Botany,* 58 (12), pp.3464-3473.

Hosoi, F., and Omasa, K., 2009. Estimating vertical plant area density profile and growth parameters of a wheat canopy at different growth stages using three-dimensional portable lidar imaging. *ISRPS Journal of Photogrammetry and Remote Sensing,* 64 (2), pp.151-158.

Hyyppä, J., Kelle, O., Lehikoinen, M., Inkinen, M., 2001. A segmentation-based method to retrieve stem volume estimates from 3-D tree height models produced by laser scanners. *IEEE Transactions on Geoscience and Remote Sensing,* 39 (5), pp.969-975.

Lefsky, M.A., Cohen, W.B., Parker, G.G., Harding, D.J., 2002. Lidar remote sensing for ecosystem studies. Bioscience 52 (1), 19-30.

Næsset, E., Gobakken, T., Holmgren, J., Hyyppä, H., Hyyppä, J., Maltamo, M., Nilsson, M., Olsson, H., Persson, Å., Söderman, U., 2004. Laser scanning of forest resources: the Nordic experience. *Scandinavian Journal of Forest Research,* 19 (6), pp.482-499.

Norman, J.M., Campbell, G.S., 1989. Canopy structure. In: Pearcy, R.W., Ehleringer, J., Mooney, H.A., Rundel, P.W. (Eds.). *Plant physiological ecology: field methods and instrumentation.* Chapman and Hall, London, pp.301-325.

Omasa, K., Akiyama, Y., Ishigami, Y., Yoshimi, K., 2000. 3-D remote sensing of woody canopy heights using a scanning helicopter-borne lidar system with high spatial resolution. *Journal of Remote Sensing Society of Japan,* 20 (4), pp.394-406.

Omasa, K., Hosoi, F., Konishi, A., 2007. 3D lidar imaging for detecting and understanding plant responses and canopy structure. *Journal of Experimental Botany,* 58 (4), pp.881-898.

Omasa, K., Qiu, G.Y., Watanuki, K., Yoshimi, K., Akiyama, Y., 2003.Accurate estimation of forest carbon stocks by 3-D remote sensing of individual trees. *Environmental Science & Technology,* 37 (6), pp.1198–1201.

Popescu, S.C., Wynne, R.H., Nelson, R.F., 2003. Measuring individual tree crown diameter with lidar and assessing its influence on estimating forest volume and biomass. *Canadian Journal of Remote Sensing,* 29(5), pp. 564–577.

Radtke, P.J., Bolstad, P.V., 2001. Laser point-quadrat sampling for estimating foliage-height profiles in broad-leaved forests. *Canadian Journal of Forest Research,* 31 (3), pp.410-418.

Ross, J., 1981. *The radiation regime and architecture of plant stands*. Dr. W. Junk, The Hague, Netherlands.

Warren-Wilson, J., 1960. Inclined point quadrats. *New Phytologist*, 59 (1), pp.1-8.